Spleen tyrosine kinase promotes NLR family pyrin domain containing 3 inflammasome-mediated IL-1β secretion via c-Jun N-terminal kinase activation and cell apoptosis during diabetic nephropathy

YINGCHUN QIAO[1*], XIXI TIAN[1*], LI MEN[1], SHENGYU LI[1], YUFENG CHEN[1], MEITING XUE[1], YAHUI HU[1], PENGFEI ZHOU[1], GUANGFENG LONG[1], YUE SHI[1], RUIQING LIU[1], YUNDE LIU[1], ZHI QI[2,3], YUJIE CUI[1,4] and YANNA SHEN[1]

[1]School of Medical Laboratory, Tianjin Medical University, Tianjin 300203; [2]Department of Histology and Embryology, School of Medicine, Nankai University, Tianjin 300071; [3]National Clinical Research Center of Kidney Diseases, Beijing 100853; [4]The Key Laboratory of Myocardial Ischemia, Harbin Medical University, Ministry of Education, Harbin, Heilongjiang 150081, P.R. China

Received December 12, 2017; Accepted May 18, 2018

DOI: 10.3892/mmr.2018.9164

Abstract. Diabetic nephropathy (DN) is a serious complication of diabetes and can cause an increased mortality risk. It was previously reported that NLR family pyrin domain containing 3 (NLRP3) inflammasome is involved in the pathogenesis of diabetes. However, the underlying mechanism is not clearly understood. In the present study, the effects of spleen tyrosine kinase (Syk) and c-Jun N-terminal kinase (JNK) on the NLRP3 inflammasome were examined *in vivo* and *in vitro*. Sprague-Dawley rats were injected intraperitoneally with streptozotocin (65 mg/kg) to induce diabetes. HK2 cells and rat glomerular mesangial cells (RGMCs) were examined to detect the expression of JNK and NLRP3 inflammasome-associated proteins following treatment with a Syk inhibitor or Syk-small interfering (si)RNA in a high glucose condition. In the present study, it was revealed that the protein and mRNA expression levels of NLRP3 inflammasome-associated molecules and the downstream mature interleukin (IL)-1β were upregulated *in vivo* and *in vitro*. The Syk inhibitor and Syk-siRNA suppressed high glucose-induced JNK activation, and subsequently downregulated the activation of the NLRP3 inflammasome and mature IL-1β in HK2 cells and RGMCs. Furthermore, high glucose-induced apoptosis of HK2 cells was reduced by the Syk inhibitor BAY61-3606. Therefore, the present results determined that high glucose-induced activation of the NLRP3 inflammasome is mediated by Syk/JNK activation, which subsequently increased the protein expression level of IL-1β and mature IL-1β. The present study identified that the Syk/JNK/NLRP3 signaling pathway may serve a vital role in the pathogenesis of DN.

Correspondence to: Professor Yujie Cui or Professor Yanna Shen, School of Medical Laboratory, Tianjin Medical University, 1 Guangdong Road, Hexi, Tianjin 300203, P.R. China
E-mail: yujiecui1@126.com
E-mail: shenyanna@sina.com

[*]Contributed equally

Key words: NLR family pyrin domain containing 3 inflammasome, spleen tyrosine kinase, c-Jun N-terminal kinase, diabetic nephropathy, apoptosis

Introduction

Diabetic nephropathy (DN) is a serious complication of diabetes and may result in end-stage renal failure (1,2). In total, ~30% of patients with diabetes mellitus (DM) developed DN following a disease duration of 15-30 years (3,4). The morbidity of DN is markedly rising with the increasing incidence and prevalence of diabetes. Albuminuria is regarded as the principal feature of DN and an independent risk factor for renal failure, in addition, hyperglycemia invariably acts as an initiating and maintaining factor during the development of end stage renal disease (5,6); however, the pathogenesis of DN has not been fully elucidated. A previous study has demonstrated that the damage of renal hemodynamics and metabolism caused by chronic hyperglycemia may lead to the secretion of inflammatory factors, followed by infiltration of immune cells (7). Therefore, the inflammatory response has been postulated to serve a key role in the pathogenesis of DN (8). A previous study conducted by Wang *et al* (9) demonstrated that inflammation is associated with DN, and overexpression of renal inflammasome components NLR family pyrin domain containing 3 (NLRP3), apoptosis-associated speck-like protein containing a CARD (ASC) and caspase-1, resulting in elevation of interleukin (IL)-1β and IL-18, subsequently contribute to renal injury. These observations suggest that the NLRP3 inflammasome may be a therapeutic target for diabetes with kidney injury.

Keller *et al* (10) demonstrated that NLRP3 is involved in the regulation of the activity of caspase-1, which in turn lead to the maturation and secretion of pro-inflammatory cytokines, including IL-1β against pathogen infection, and may additionally drive pyroptosis (3). The c-Jun N-terminal kinase (JNK) signaling pathway is activated through lysosome rupture, which subsequently leads to the complete activation of the NLRP3 inflammasome in macrophages (11). It was hypothesized that high glucose may induce activation of the JNK signaling pathway. In the present study, it was demonstrated that JNK, a stress-responsive mitogen-activated protein kinase, was activated following high glucose stimulation and a JNK inhibitor suppressed NLRP3 inflammasome activation.

Spleen tyrosine kinase (Syk) is a non-receptor protein tyrosine kinase, which transmits B-cell antigen receptor or Fc-receptor signaling of hematopoietic cells, and Syk may result in gene transcriptions of C-C motif chemokine ligand 2 and transforming growth factor β-1, which may be involved in the development of DN (12). It was additionally observed that a tyrosine phosphorylation site is on ASC acts as a molecular switch controlling inflammasome assembly (3,7). In the present study, it was demonstrated that Syk was involved in JNK-dependent NLRP3 inflammasome activation in high glucose-induced HK2 cells and rat glomerular mesangial cells (RGMCs).

Materials and methods

Animals. Sixty Male Sprague-Dawley rats (age, 5-week-old; weight, 180-200 g) were purchased from The Laboratory Animal Center of the Academy of Military Medical Sciences (Beijing, China). They were maintained under standard conditions of temperature (23±5˚C) and humidity (60±5%) with an alternating 12 h light/dark cycles. All the animals had access to clean drinking water and a standard pellet diet. The rats in the experimental group (n=36) were given a single intraperitoneal injection of fresh streptozotocin (STZ; 65 mg/kg; Sigma-Aldrich; Merck KGaA) in 0.1 M sodium citrate buffer (pH 4.3); whereas, the control group rats (n=24) received the same dosage of sodium citrate buffer only. At 72 h following injection, blood glucose ≥16.7 mM was considered as diabetes. The body and kidney weight, blood and urine glucose and albumin were determined at week 12 and 16. Seven DN and six control rats were sacrificed at 12, 16, 20 and 33 weeks, respectively, and kidneys were analyzed for mRNA and protein expression at 12, 16, 20 and 33 weeks. All the experimental procedures in the present study were approved by the Animal Care and Welfare Committee of Tianjin Medical University (Tianjin, China).

Reagents and antibodies. NLRP3 (cat. no. 13158, 1:1,500), phosphorylated (p)-Syk (cat. no. 2710, 1:1,500), p-JNK (cat. no. 9255, 1:1,500), Syk (cat. no. 13198, 1:1,500), JNK (cat. no. 9252, 1:1,500), and cleaved caspase-1 (cat. no. 4199, 1:1,500) antibodies were obtained from Cell Signaling Technology, Inc. (Danvers, MA, USA); caspase-1 (cat. no. ab179515, 1:1,500), pro-IL-1β (cat. no. ab2105, 1:2,000) and mature (m)IL-1β (cat. no. ab9722, 1:2,000) antibodies from Abcam (Cambridge, UK); apoptosis regulator Bax (cat. no. 200958, 1:1,000) and Bcl-2 (cat. no. 230004, 1:500) apoptosis regulator (Bcl-2; BH3 Domain Specific) antibodies from Zen BioScience (Chengdu, China); ASC (cat. no. sc-271054, 1:500); β-actin (cat. no. sc-47778, 1:1,000) and mouse anti-rabbit IgG-HRP (cat. no. sc-2357, 1:4,000) antibodies from Santa Cruz Biotechnology, Inc. (Dallas, TX, USA); anti-mouse IgG HRP Conjugate (cat. no. W4021, 1:5,000) from Promega (Madison, WI, USA). All cell culture reagents were obtained from Thermo Fisher Scientific, Inc. (Waltham, MA, USA). JNK inhibitor II was purchased from Merck KGaA (Darmstadt, Germany), and Syk inhibitor IV, BAY61-3606 from Santa Cruz Biotechnology, Inc. The radioimmunoprecipitation assay lysis buffer [50 mM Tris (pH 7.4), 150 mM NaCl, 1% Triton X-100, 1% sodium deoxycholate, 0.1% SDS] was purchased from Beyotime Institute of Biotechnology (Haimen, China). TRIzol® reagent was obtained from Thermo Fisher Scientific, Inc. The fluorescein iosthiocyanate (FITC)-Annexin V Apoptosis Detection kit was obtained from BioLegend, Inc. (London, UK). Lipofectamine® 3000 was purchased from Invitrogen (Thermo Fisher Scientific, Inc.) Small interfering (si)RNA specific to Syk was purchased from Santa Cruz Biotechnology, Inc.

Cell culture. The HK2 cell line was derived from a normal adult human kidney (13) and RGMC was derived from rat renal glomeruli (14). In the present study, the HK2 cells (cat. no. ZQ0313) and RGMCs (HBZY-1; cat. no. ZQ0540) were purchased from Shanghai Zhong Qiao Xin Zhou Biotechnology Co., Ltd. (Shanghai, China). HK2 cells were maintained in Dulbecco's modified Eagle's medium (DMEM)/F-12 (1:1) basic (1X) medium (Thermo Fisher Scientific, Inc.) supplemented with 10% fetal bovine serum (FBS, Gibco; Thermo Fisher Scientific, Inc.), 1% streptomycin/penicillin. RGMCs were cultured in DMEM containing 5 mM glucose and 10% FBS at 37˚C and 5% CO_2. The cells were added to the 6-well plate at a density of $1x10^6$ cells/well and treated with 5 or 25 mM glucose or high mannitol (Mtol) concentration (5 mM glucose + 20 mM Mtol), then pretreated with Syk inhibitor (1 μM) or Syk-siRNA for 12, 24, 36 and 48 h to detect the expression of the NLRP3 inflammasome or for 10, 20, 30 and 40 min to detect the protein level of p-JNK.

Transient transfection. siRNA (50 nM) specific to Syk (Syk-siRNA) was used to knockdown Syk and a scramble siRNA, termed negative control (NC)-siRNA, was used as a control in the experiment. HK2 cells and RGMCs were transfected using Lipofectamine® 3000 reagent following the manufacturer's protocol. Sequences for Syk-siRNA were as follows: Sense, 5'-GCAUGAGUGAUGGGCUUU ATT-3'; antisense, 5'-UAAAGCCCAUCACUCAUGCTT-3'. Sequences for NC-siRNA as follows: Sense, 5'-UUCUCC GAACGUGUCACGUTT-3'; antisense, 5'-ACGUGACAC GUUCGGAGAATT-3'. Following 48 h of transfection, the cells were treated with the high glucose and harvested for western blotting.

Histological examination. For histological assessment, the renal cortex was fixed in 4% neutral buffered paraformaldehyde for 24 h at 4˚C, embedded in paraffin and cut to 5-μm sections. The sections were dewaxed using standard sequential techniques at room temperature. Some sections were stained with hematoxylin and eosin (H&E), the slides were dipped consecutively in 100, 90, 70 and 50% alcohol for 2 min each, and placed over running tap water for 10 min before and after dipping in haematoxylin for 10-15 min. The slides were dipped twice in 1% acid alcohol and again placed over running tap water for 10 min before and after dipping twice in 1% ammonia solution. Finally, the slides were dipped in 2% eosin solution for 2-3 min and washed with absolute alcohol twice. The slides were mounted in mounting medium (Solarbio, China) and observed under a light microscope.

For periodic acid-Shiff (PAS) staining, the formaldehyde sections were dewaxed, hydrated, stained with schiff's reagent for 10-15 min at room temperature, then washed with running water for 5 min. The sections were re-dyed with hematoxylin for 1-2 min, then washed and soaked in 1% acetic acid aqueous solution for 3-5 sec, differentiated with 1% acidified ethanol for 3-5 sec at room temperature to remove the excessive binding dyes, stained with aniline blue for 5 min at room temperature, immersed in 0.2% acetic acid aqueous solution for 3-5 sec, treated with 95% ethanol and absolute ethanol, cleared with xylene, and mounted with neutral gum. A total of 10 fields were randomly observed using a light microscope (magnification, x200 and x400).

Immunohistochemistry. Sections were permeabilized with 1% Triton X-100 for 2 h and blocked with normal goat serum (Beyotime Institute of Biotechnology, Haiman, China) for 30 min at room temperature, the sections were incubated sequentially with NLRP3 (1:500; cat. no. ab223687; Abcam), caspase-1 (1:500; cat. no. ab108362; Abcam) and mIL-1β (1 μg/ml; cat. no. ab9722; Abcam) antibodies at 4˚C overnight. The next day, after rewarming for 1 h, sections were washed with PBS and then incubated with mouse anti-rabbit IgG-HRP (cat. no. sc-2357, 1:100) antibody for 2 h at room temperature. To visualize the signals, sections were treated with peroxidase substrate 3,3'-diaminobenzidine (DAB, 0.05%, ZSGB-Bio, China) and counterstained with hematoxylin for 1 min at room temperature. Sections were viewed and imaged under a light microscope (Ni-U; Nikon Corporation, Tokyo, Japan). Images were analyzed quantitatively using Image-Pro Plus 6.0 (Media Cybernetics, Inc., Rockville, MD, USA).

Western blot analysis. The renal cortex was excised and homogenized in protein extraction buffer and centrifuged at 13,000 x g, 4˚C for 20 min. Protein concentration of the supernatants of tissue homogenate, HK2 cells and RGMCs were measured using a bicinchoninic acid protein assay kit. 25 μg protein was loaded per lane and separated on 10 or 12% SDS-PAGE and transferred to polyvinylidene difluoride membranes. Following blocking with 5% fat-free dry milk or BSA for 2 h at room temperature, the membranes were incubated with the primary antibody (mentioned above) overnight at 4˚C. Following three washes with Tris-buffered saline/Tween 20, the membranes were probed with secondary antibodies [anti-mouse immunoglobulin G (IgG) or anti-rabbit IgG] at room temperature for 1 h. The protein bands were visualized with a Horseradish Peroxidase Substrate Peroxide Solution (EMD Millipore, Billerica, MA, USA) and quantified using ImageJ software 6.0 (National Institutes of Health, Bethesda, MD, USA).

Reverse transcription-polymerase chain reaction (RT-PCR). To measure specific gene expression, the primer sequences for NLRP3, caspase-1 and IL-1β were synthesized (Table I). Total RNA of rat renal cortex from the control group and DM group was isolated using TRIzol® reagent, according to the manufacturer's protocol. RT (42˚C for 1 h; 70˚C for 5 min) was conducted using the TIANGEN RNA PCR kit (Tiangen Biotech Co., Ltd., Beijing, China). The DNA polymerase was purchased from Invitrogen (Thermo Fisher Scientific, Inc.). PCR reactions were performed at an initial denaturation at 94˚C for 3 min, followed by 35 cycles at 94˚C for 30 sec, 55/59/60˚C for 30 sec, 72˚C for 1 min and final extension step at 72˚C for 5 min. The amplified products were detected by 1.5% agarose gel electrophoresis, stained with ethidium bromide (0.5 μg/ml) for 40 min at room temperature. Gene expression was normalized to β-actin by ImageJ software 6.0 (National Institutes of Health).

Flow cytometry. The cells were treated with BAY61-3606 for 2 h, followed by high glucose treatment for 36 h, and washed twice with cold Cell Staining Buffer (BioLegend, Inc.). Subsequently, cells were resuspended in annexin V binding buffer at a density of 0.25-1.00x10^7 cells/ml and added 5 μl FITC-annexin V and 10 μl propidium iodide solution, then placed at room temperature for 15 min in the dark. Annexin V binding buffer (400 μl) was added to each tube and analyzed using a flow cytometer. All data were analyzed using FlowJo software 7.6 (FlowJo LLC, Ashland, OR, USA), according to the manufacturers' protocol.

Statistical analysis. Data are presented as the mean ± standard error of the mean. At least three independent experiments and differences between groups were analyzed by GraphPad Prism 5 software (GraphPad Software, Inc., La Jolla, CA, USA). Student's t-test was used for comparison between two groups. One-way analysis of variance was used followed by Dunnett's post hoc test for comparing between all columns and control column, or Tukey's post hoc test for comparing all pairs of columns. $P<0.05$ was considered to indicate a statistically significant difference.

Results

Rat model of DN. The body weight, blood glucose and urine glucose of the diabetic rats were significantly increased compared with the corresponding control rats (Table II; $P<0.001$). Additionally, urine amount and albumin excretion were significantly increased compared with the control groups (Table II; $P<0.01$), which indicated the dysfunction of kidneys of diabetic rats. Furthermore, PAS and H&E staining for the kidneys demonstrated glomerular hypertrophy and mesangial expansion in the diabetic rats (Fig. 1). In contrast, these alterations were not observed in the rats of the control

Table I. Primers for reverse transcription-polymerase chain reaction.

Gene	Forward sequence (5'-3')	Reverse sequence (5'-3')
NLR family pyrin domain containing 3	AGGGCTCTGTTCATTG	CTTCCACGTCTCGGTTC
Caspase-1	TGCCTGGTCTTGTGACTTGGAG	ATGTCCTGGGAAGAGGTAGAAACG
Interleukin-1β	TGGGATGATGACGACCTGC	GGAGAATACCACTTGTTGGCTTA
β-actin	GTTGACATCCGTAAAGACC	GACTCATCGTACTCCTGCTC

Table II. The renal function parameters of streptozotocin-induced diabetic rats.

	12 weeks		16 weeks	
Parameters	Control	Diabetes	Control	Diabetes
Body weight (g)	516.3±11.20	236.7±17.32[c]	624.3±1.202	329.0±24.06[c]
Kidney/body weight ratio (%)	0.27±0.030	0.59±0.037[b]	0.30±0.0053	0.56±0.00[a]
Blood glucose (mmol/l)	6.26±0.27	32.27±0.61[c]	6.07±0.43	32.70±0.30[c]
Urine amount (ml)	10.67±3.18	198.3±22.28[b]	11.20±2.88	250.8±17.15[c]
Urine glucose (mmol/l)	2.45±0.13	357.2±28.89[c]	3.03±0.91	425.1±32.20[c]
Albumin excretion (mg/24 h)	21.63±5.17	140.3±17.45[b]	14.16±3.721	100.3±6.86[c]

Data are presented as the mean ± standard error of the mean. n=3/group. Statistical significance was determined using the Student's t-test. [a]P<0.05, [b]P<0.01, [c]P<0.001 vs. respective control.

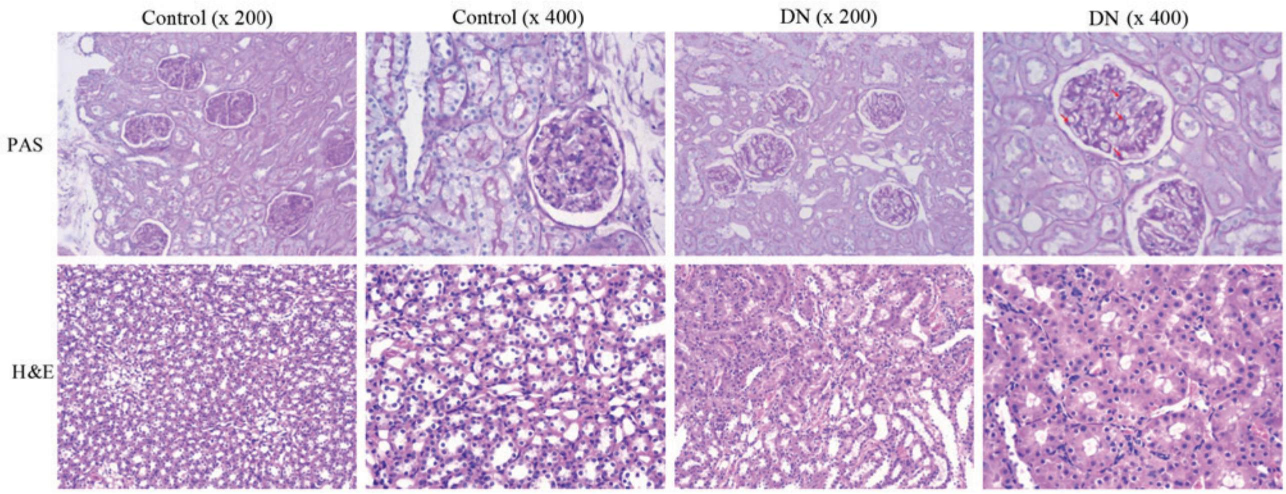

Figure 1. Streptozotocin-induced DN in rats. Histological examination by PAS staining and H&E staining (x200 and x400 magnification) for DN rats at 12 weeks. The arrowheads represent the sections of expanding glomerular basement membrane. DN, diabetic nephropathy; PAS, periodic acid-Shiff; H&E, hematoxylin and eosin.

group, suggesting that the renal structure of diabetic rats was disorganized.

NLRP3 inflammasome is activated in rats with DN. Previous studies reported that inflammasome activation participates in the development of DN; therefore, the renal injury was estimated by immunohistochemical staining of NLRP3, caspase-1 and mIL-1β. As demonstrated in Fig. 2A and B, the expression of NLRP3, caspase-1 and mIL-1β in the DN group was significantly higher compared with the control group (P<0.01). Protein expression levels of NLRP3 inflammasome was examined in DN rat kidneys at different weeks, but its protein expression levels at 16 weeks was upregulated more. Furthermore, there was no difference in the expression levels of NLRP3 inflammasome in control rats at different weeks. Therefore, the 16-week-old DN and control rats was chosen as the experimental time point. Three different rats from the control group at 16 weeks (termed C1, C2 and C3) and three different rats from the DN group at 16 weeks (termed DN1, DN2 and DN3) was selected to assess the

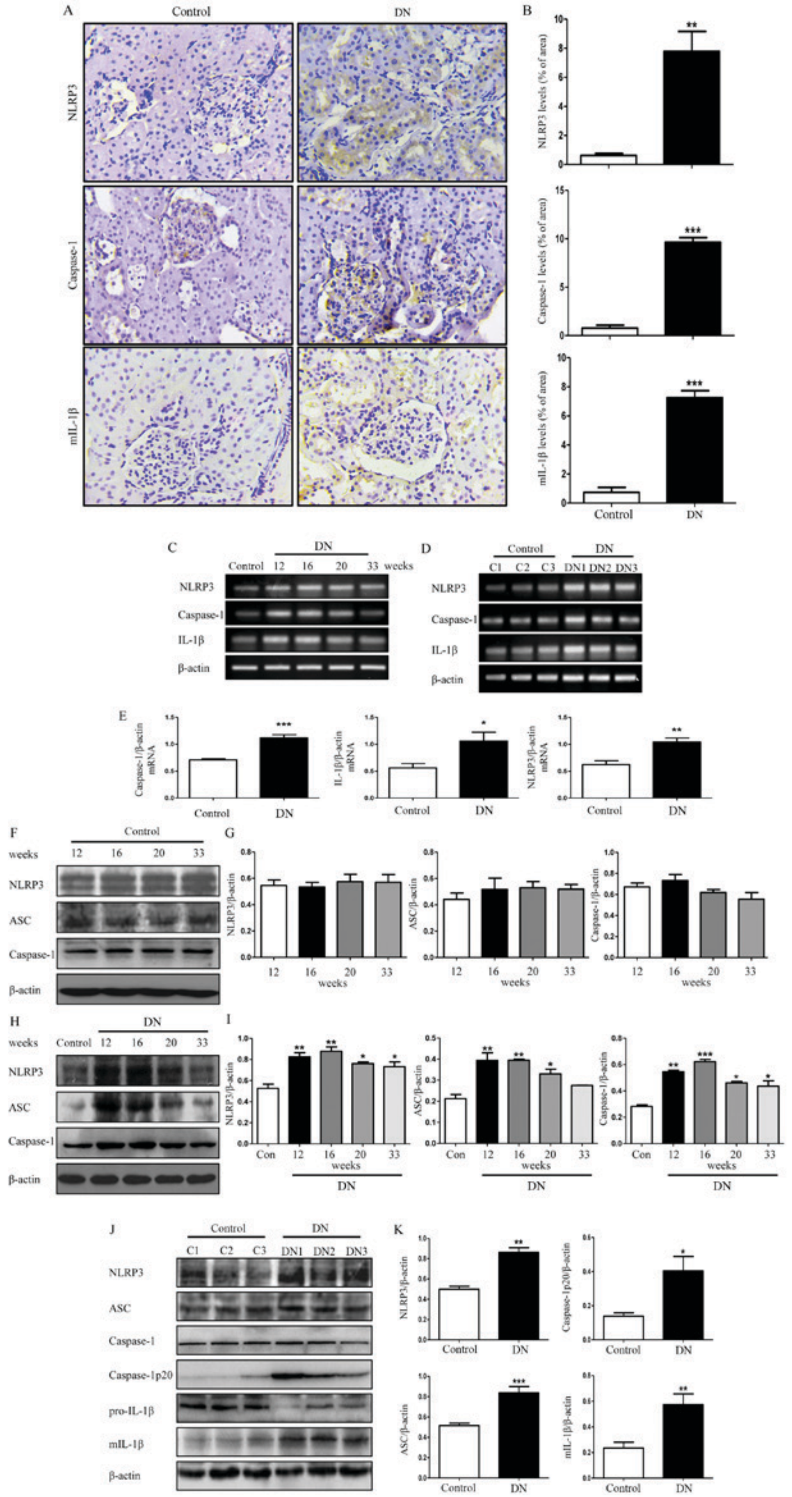

Figure 2. NLRP3 inflammasome activity in DN rats. (A) Representative images of paraformaldehyde-fixed kidney sections from the control group and DN group rats at 16 weeks were stained with anti-NLRP3, anti-caspase-1 and anti-mIL-1β antibodies and representative images (x400x magnification). (B) Staining of NLRP3, caspase-1, mIL-1β in rat kidney was quantified using Image-Pro Plus 6.0. (C) Total RNA from the kidneys of the 16-week-old control rats and DN rats was extracted and subjected to RT-PCR for NLRP3, caspase-1 and IL-1β at 12, 16, 20 and 33 weeks. (D) RNA was extracted from kidneys of three different control rats and three different DN rats, and then subjected to RT-PCR at week 16. (E) Densitometry analysis of the mRNA levels of NLRP3, caspase-1 and IL-1β in 16-week-old control rat kidneys and DN rat kidneys. (F) Total lysates from kidneys in control rats at different weeks were extracted and subjected to western blot analysis for NLRP3, ASC and caspase-1. (G) Densitometry analysis of NLRP3, ASC and caspase-1 in. (H) The protein expression levels of NLRP3, ASC and caspase-1 in DN rats at 12, 16, 20 and 33 weeks and control rats at 16 weeks. (I) Densitometry analysis of NLRP3, ASC and caspase-1. (J) Protein was extracted from kidneys of three different DN rats and three different control rats, and then subjected to western blot to detect the protein levels of these molecules mentioned above in 16-week-old DN and control rats. (K) Densitometry analysis of NLRP3, ASC, caspase-1p20 and mIL-1β. Data are presented as the mean ± standard error of the mean from three independent experiments. Student's t-test was used for comparison between control group and DN group (for A-E, J and K). One-way ANOVA followed by Dunnett's post hoc (for H and I) or Tukey's post hoc test (F and G). *P<0.05, **P<0.01, ***P<0.001 vs. control group. β-actin was used as the internal loading control. RT-PCR, reverse transcription-polymerase chain reaction; ANOVA, analysis of variance; DN, diabetic nephropathy; NLRP3, NLR family pyrin domain containing 3; mIL-1β, mature interluekin-1β; C, control; ASC, apoptosis-associated speck-like protein containing a CARD.

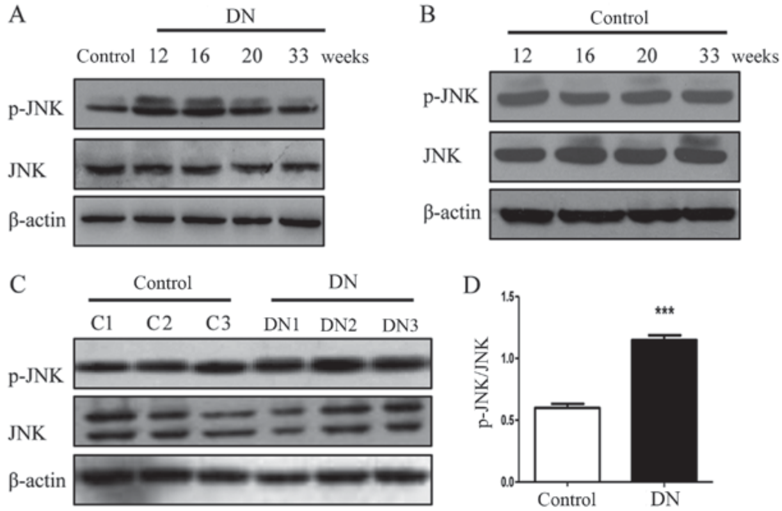

Figure 3. Activation of JNK in DN rats. (A) Phosphorylation of JNK in the kidneys of DN rats at week 12, 16, 20, 33 and control rats at week 16. (B) Phosphorylation of JNK in the kidneys of the control rats at 12, 16, 20 and 33 weeks. (C) Level of p-JNK in three different DN rats and three different control rats at week 16 were detected by western blotting. (D) Quantification of the JNK expression. Data are presented as the mean ± standard error of the mean from three independent experiments. Statistical significance was determined using the Student's t-test. ***P<0.001 vs. control. p, phosphorylated; JNK, c-Jun N-terminal kinase; DN, diabetic nephropathy; C, control.

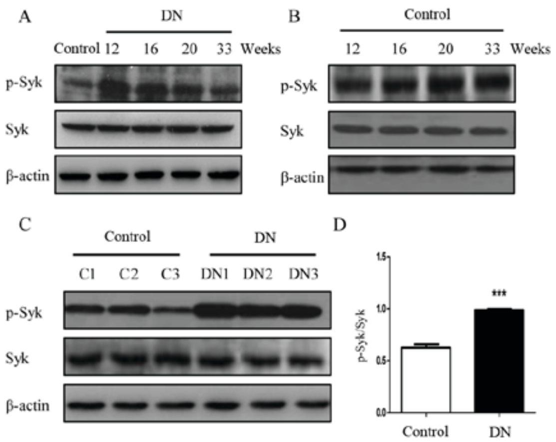

Figure 4. Role of Syk in DN rats. The protein expression level of p-Syk and Syk was examined in the kidneys of (A) control rats at 16 weeks and DN rats at different weeks as well as. (B) control rats at different weeks. (C) Phosphorylation of Syk in three different DN rats and three different control rats at week 16 and (D) densitometry analysis of p-Syk. Data are presented as the mean ± standard error of the mean from at least three independent experiments. Statistical significance was determined using the Student's t-test. ***P<0.001 vs. control. DN, diabetic nephropathy; p, phosphorylated; Syk, spleen tyrosine kinase; C, control.

mRNA expression levels of NLRP3 in kidney tissues (Fig. 2C-E). There was an ~2 fold increase in the expression level of NLRP3 in the diabetic rats group compared with the control group (Fig. 2E; P<0.01). Furthermore, the mRNA expression levels of caspase-1 and IL-1β were also significantly increased (Fig. 2E; P<0.05).

The protein expression levels of NLRP3 inflammasome-associated molecules in the control group were detected at 12, 16, 20 and 33 weeks, and normalized to β-actin as a control. It was identified that there was no alteration in the expressions of these molecules in the control group at different weeks (Fig. 2F and G), thus we randomly selected the 16-week-old control rats as the control group for our further examination. We detected the protein level of NLRP3 inflammasome in the DN rat kidneys and the result revealed that the protein expression levels of NLRP3, ASC and caspase-1 in the DN rats at 12, 16, 20 and 33 weeks were significantly increased compared with the control group rats at 16 weeks (Fig. 2H and I; P<0.05) with the exception of ASC at week 33. Among them, the most marked difference in expression was observed in 16-week-old rats (Fig. 2H and I); therefore, we selected the 16-week-old DN rats as our experimental group for further examination. Three different rats from the control group at 16 weeks (C1, C2 and C3) and three different rats from the DN group at 16 weeks (DN1, DN2 and DN3) were selected for further evaluation. As demonstrated in Fig. 2J and K, in addition to upregulation of NLRP3, the expression of caspase-1p20, an active form of caspase-1, was significantly higher compared with the control group (Fig. 2K; P<0.05). Simultaneously, the protein expression level of mIL-1β was significantly increased (Fig. 2K; P<0.01).

Phosphorylation of JNK is increased in rats with DN. In a similar trend to the NLRP3 inflammasome-associated molecules, the phosphorylation of JNK was increased in the diabetic rats at 12, 16, 20 and 33 weeks (Fig. 3A and B) and the phosphorylation levels of JNK in the three 16-week-old DN rats (DN1, DN2 and DN3) were significantly increased compared with the three 16-week-old rats (C1, C2 and C3) in the control group (P<0.001; Fig. 3C and D). These results suggest that JNK is involved in the pathogenesis of DN.

Syk is activated in rats with DN. To determine whether Syk is involved in the pathogenesis of DN, the protein expression of Syk was detected in renal tissue. Western blot analysis demonstrated that level of p-Syk in the diabetic group rats appeared increased compared with the control group at the corresponding 12, 16, 20 and 33 weeks (Fig. 4 and B). Further confirming these observations, phosphorylation of Syk in the three different 16-week-old DN rats (DN1, DN2 and

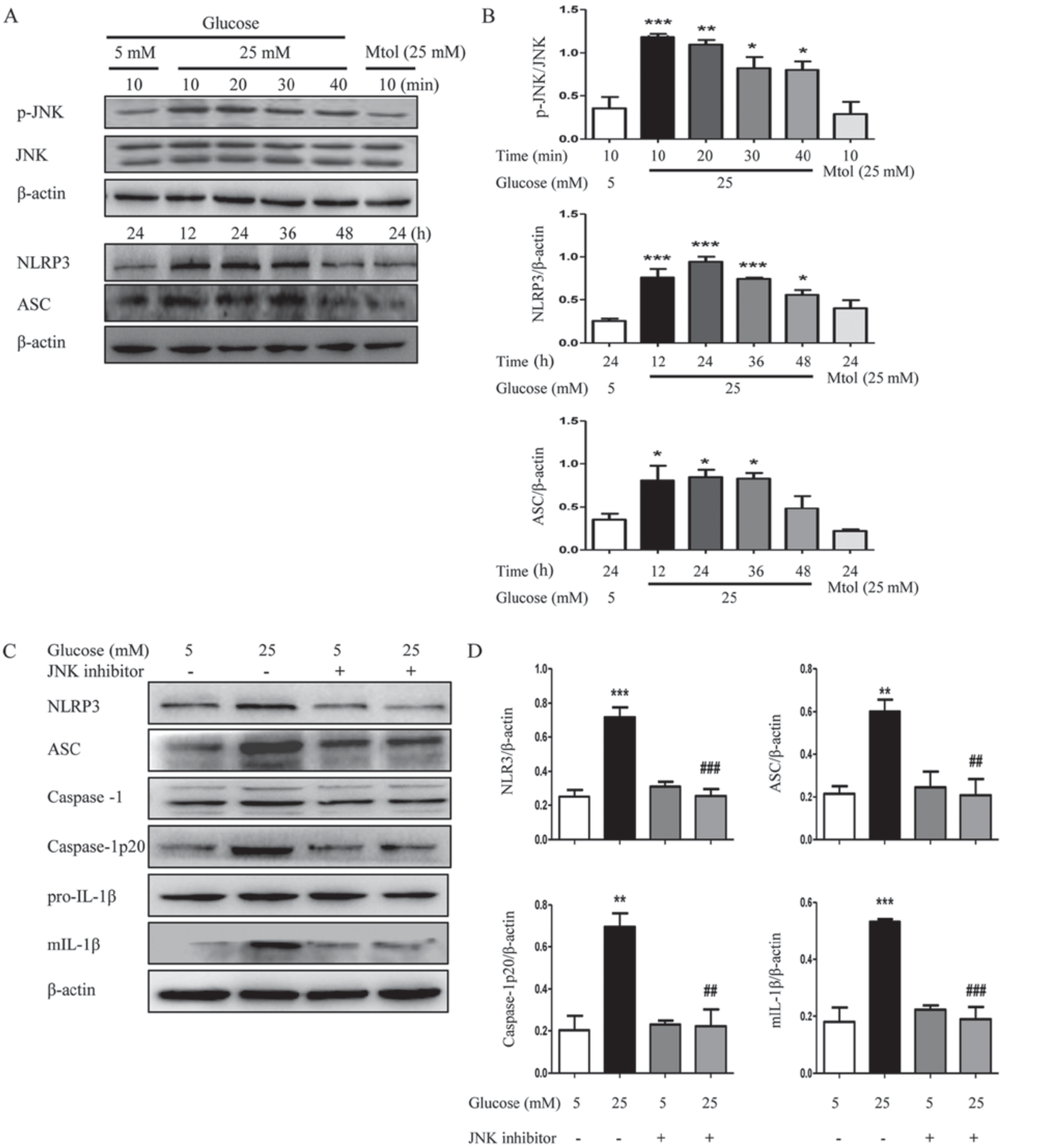

Figure 5. Inhibition of JNK suppresses NLRP3 inflammasome activation in HK2 cells. (A) HK2 cells were cultured in Dulbecco's modified Eagle's medium/F12 (1:1) containing 5 mM glucose or 25 mM glucose for different times. The protein expression levels of p-JNK, NLRP3 and ASC were detected by western blotting. (B) Densitometry analysis of p-JNK, NLRP3 and ASC. (C) The protein expression levels of NLRP3, ASC, caspase-1, caspase-1p20, pro-IL-1β and mIL-1β of HK2 cells were detected by western blotting following treatment with JNK inhibitor (10 μM) and (D) densitometry analysis was performed. The data are presented as the mean ± standard error of the mean of three independent experiments. Statistical significance was determined by one-way analysis of variance followed by Dunnett's post hoc test (for A and B) or Tukey's post hoc test (for C and D). *P<0.05, **P<0.01, ***P<0.001 vs. 5 mM glucose. ##P<0.01, ###P<0.001 vs. 25 mM glucose. Mtol, mannitol; p, phosphorylated; JNK, c-Jun N-terminal kinase; NLRP3, NLR family pyrin domain containing 3; ASC, apoptosis-associated speck-like protein containing a CARD; mIL-1β, mature interleukin 1β.

DN3) kidney was significantly increased compared with the three 16-week-old rats (C1, C2 and C3) in the control group (P<0.001; Fig. 4C and D).

Inhibition of JNK attenuates high glucose-induced NLRP3 inflammasome activation in HK2 cells. To confirm the role of JNK, HK2 cells were treated with or without the JNK inhibitor (10 μM) for 2 h, and subsequently exposed to 5 or 25 mM glucose for 24 h. As demonstrated in Fig. 5A and B, high glucose (25 mM) induced a significant increase in the phosphorylation level of JNK, particularly at 10 and 20 min, compared with normal glucose (P<0.01). Furthermore, the

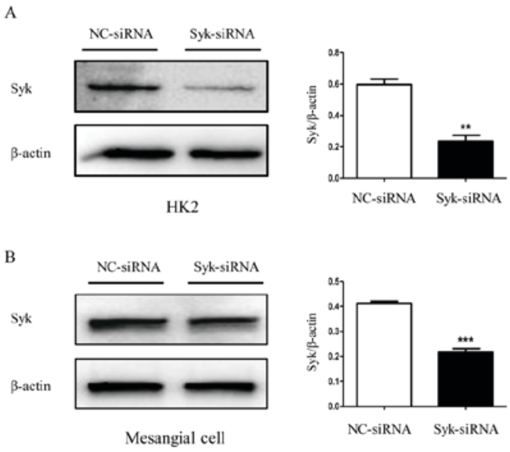

Figure 6. Interference effect of Syk-siRNA in HK2 cells and RGMCs. (A) HK2 cells transfected for 48 h with either NC-siRNA or Syk-siRNA. (B) RGMCs transfected for 48 h with either NC-siRNA or Syk-siRNA. β-actin was used as an internal control. **P<0.01, **P<0.001 vs. Control group.

protein expression levels of NLRP3 and ASC were also increased subsequent to treatment with high glucose, particularly at 12, 24 and 36 h. The JNK inhibitor downregulated the high glucose-induced increased expression of NLRP3, caspase-1p20 and ASC expression and along with a decrease in the maturation of IL-1β (Fig. 5C and D), confirming that JNK may have a critical role in NLRP3-dependent maturation of IL-1β during the development of DN.

Syk is involved in JNK-dependent NLRP3 inflammasome activation in high glucose-induced HK2 cells and RGMCs. The role of Syk in JNK-dependent NLRP3 inflammasome activation induced by high glucose was further investigated. The protein level of Syk in HK2 cells and RGMCs was evaluated following transfection with Syk-siRNA. As expected, Syk protein levels were significantly decreased by Syk-siRNA transfection compared with control (Fig. 6A and B). As demonstrated in Fig. 7A, phosphorylation of Syk was increased following treatment with high glucose, significantly at 10 and 20 min compared with normal glucose levels (P<0.05). By contrast, the hyperosmotic Mtol control group exhibited no effect on the production of p-Syk in HK2 cells. In Fig. 7B, high glucose increased the phosphorylation of JNK and the addition of BAY61-3606 decreased high glucose-induced phosphorylation of JNK. The increased protein expression of downstream molecules, including NLRP3, ASC, caspase-1p20 and mIL-1β induced by high glucose was significantly reduced following Syk inhibition (Fig. 7C and D; P<0.05). The addition of Syk-siRNA demonstrated a similar effect. The expression of p-JNK and NLRP3 inflammasome was markedly decreased in Syk-siRNA-treated HK2 cells compared with high glucose-treated HK2 cells (Fig. 7E-G), which suggests an important role of Syk in regulating JNK-dependent activation of NLRP3 inflammasome and subsequent maturation of IL-1β upon stimulation with high glucose.

It was additionally demonstrated that Syk had a critical role in the JNK/NLRP3/IL-1β pathway in high glucose induced RGMCs. As demonstrated in Fig. 8A-C, the Syk inhibitor BAY61-3606 significantly decreased the level of p-JNK and the downstream molecules, including NLRP3, ASC, caspase-1p20 and mIL-1β, induced by high glucose (P<0.05). Similar effects were also observed in Syk-siRNA-treated cells (Fig. 8D-F). Taken together, these data demonstrated that Syk acts upstream of JNK and NLRP3 inflammasome in RGMCs.

Syk is involved in high glucose-induced apoptosis of HK2 cells. The aforementioned results collectively support that Syk is involved in the process of apoptosis; to verify the implication of Syk in the pathomechanism of apoptosis in DN, a series of experiments were performed. HK2 cells were pretreated with high glucose for 36 h and the protein expression levels of Bax and Bcl-2 were subsequently determined by western blotting. As demonstrated in Fig. 9A, expression of Bax was significantly increased and Bcl-2 significantly decreased by high glucose (P<0.001). Furthermore, high glucose-induced activation of Bax was decreased and Bcl-2 was increased in HK2 cells upon incubation with the Syk inhibitor BAY61-3606 (Fig. 9B). Additionally, the flow cytometry analysis demonstrated that the inhibition of Syk significantly reduced apoptosis of HK2 cells in high glucose (Fig. 9C). Although the apoptotic rate of HK2 cells in 5 mM glucose+BAY61-3606 treated group was higher than that in 5 mM glucose treated group, that was not statistically significant (data not shown). Taken together, these results indicated that Syk was involved in high glucose-induced apoptosis of HK2 cells; however, the specific mechanism requires further investigation.

Discussion

DN is a serious complication of DM, with 25-40% of patients with type 1 DM developing DN within 20-25 years of diabetes and leads to a high mortality rate worldwide (15). Therefore, finding novel therapeutic strategies against DN is an important unmet medical requirement at present (16). Previous studies reported that the immune-mediated inflammatory response participates in the development of DN. Numerous inflammatory cytokines, including IL-1β, IL-18, tumor necrosis factor-α, C-C motif chemokine 2 and intercellular adhesion molecule 1 are significantly increased in renal tissues during DN and attenuating the expression of these cytokines may protect against diabetic renal injury (17-19). In the present study, it was demonstrated that the expression of NLRP3 was upregulated in high-glucose induced HK2 cells, which also led to upregulation of ASC expression, cleavage of caspase-1 and maturation of IL-1β. Furthermore, it was identified that the phosphorylation levels of Syk and JNK were significantly increased in the DN kidneys compared with control animals. While, the increase in phosphorylation of Syk and JNK appears to have been diminished over time. Kanellis *et al* (20) demonstrated that in I/R rat kidneys, delaying JNK inhibitor treatment until 1 h following reperfusion conferred no benefit, combined with the present results, it may suggest that the early peak of JNK activation is the main pathologic event during kidney injury. To examine the effects of Syk on the inflammasome pathway during the pathogenesis of DN, the core inflammatory molecular expression was investigated in HK2 cells and RGMCs. BAY61-3606 inhibited JNK-mediated

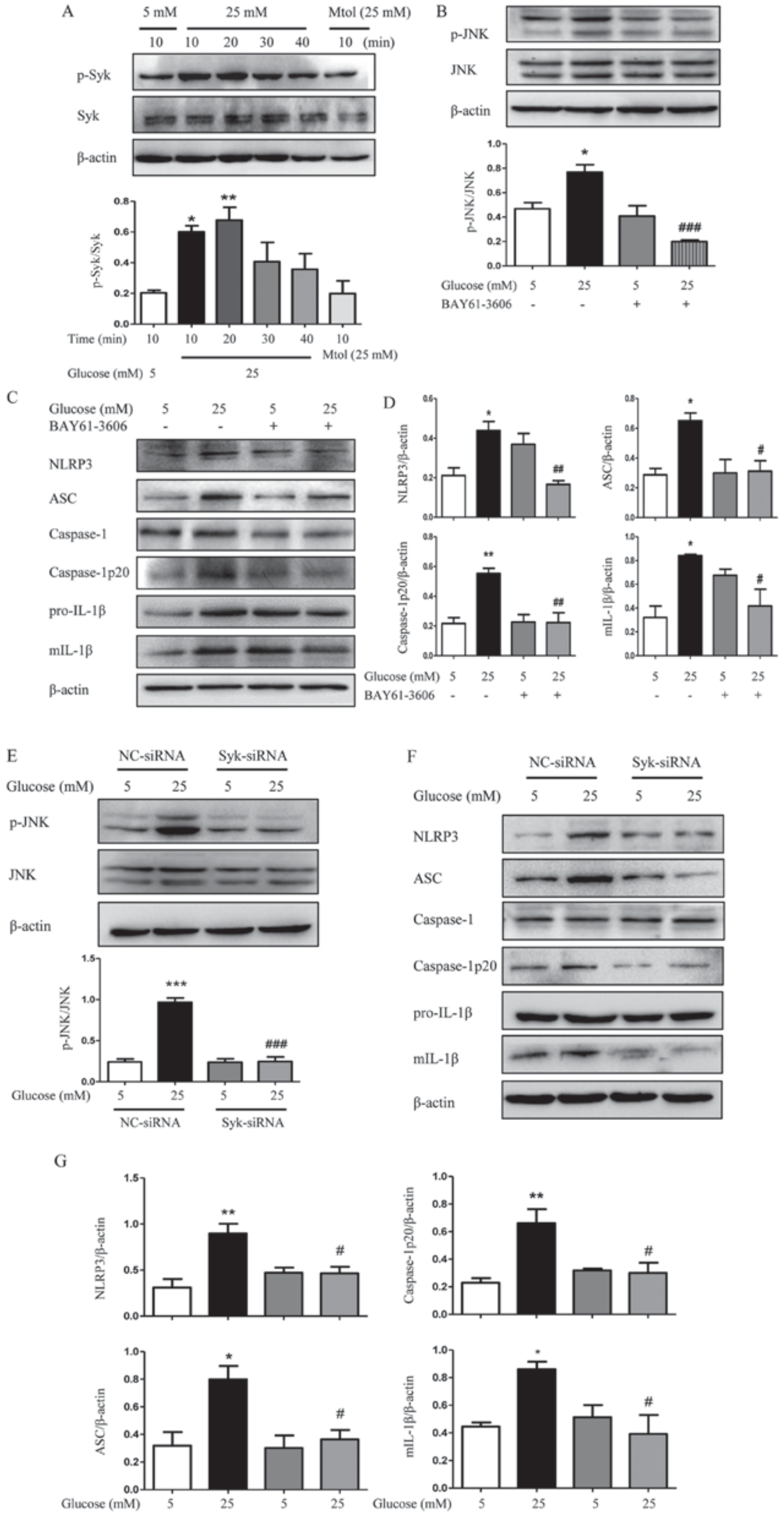

Figure 7. Syk is involved in JNK-dependent NLRP3 inflammasome activation in high glucose-induced HK2 cells. (A) Level of p-Syk was determined in HK2 cells. (B) Effects of BAY61-3606 on high glucose-induced phosphorylation of JNK determined by western blotting. (C) Protein expression level of NLRP3, ASC, caspase-1, caspase-1p20, pro-IL-1β and mIL-1β were examined by western blotting in HK2 cells and (D) analyzed using densitometry. (E) HK2 cells transfected with siRNA against Syk were exposed to high glucose condition for 48 h and the expression of p-JNK was measured and quantified. (F) HK2 cells were additionally examined to determine the protein expression levels of NLRP3, ASC, caspase-1, caspase-1p20, pro-IL-1β and mIL-1β by western blotting and (G) densitometry was performed using ImageJ software. The data are presented as the mean ± standard error of the mean of three independent experiments. *P<0.05, **P<0.01 vs. 5 mM glucose by one-way ANOVA followed by Dunnett's post hoc test (for A). #P<0.05, ##P<0.01, ###P<0.001 vs. 25 mM glucose by one-way ANOVA followed by Tukey's post hoc test (for B-G). ANOVA, analysis of variance; NC, negative control; siRNA, small interfering RNA; Syk, spleen tyrosine kinase; p, phosphorylated; JNK, c-Jun N-terminal kinase; NLRP3, NLR family pyrin domain containing 3; ASC, apoptosis-associated speck-like protein containing a CARD; mIL-1β, mature interleukin 1β.

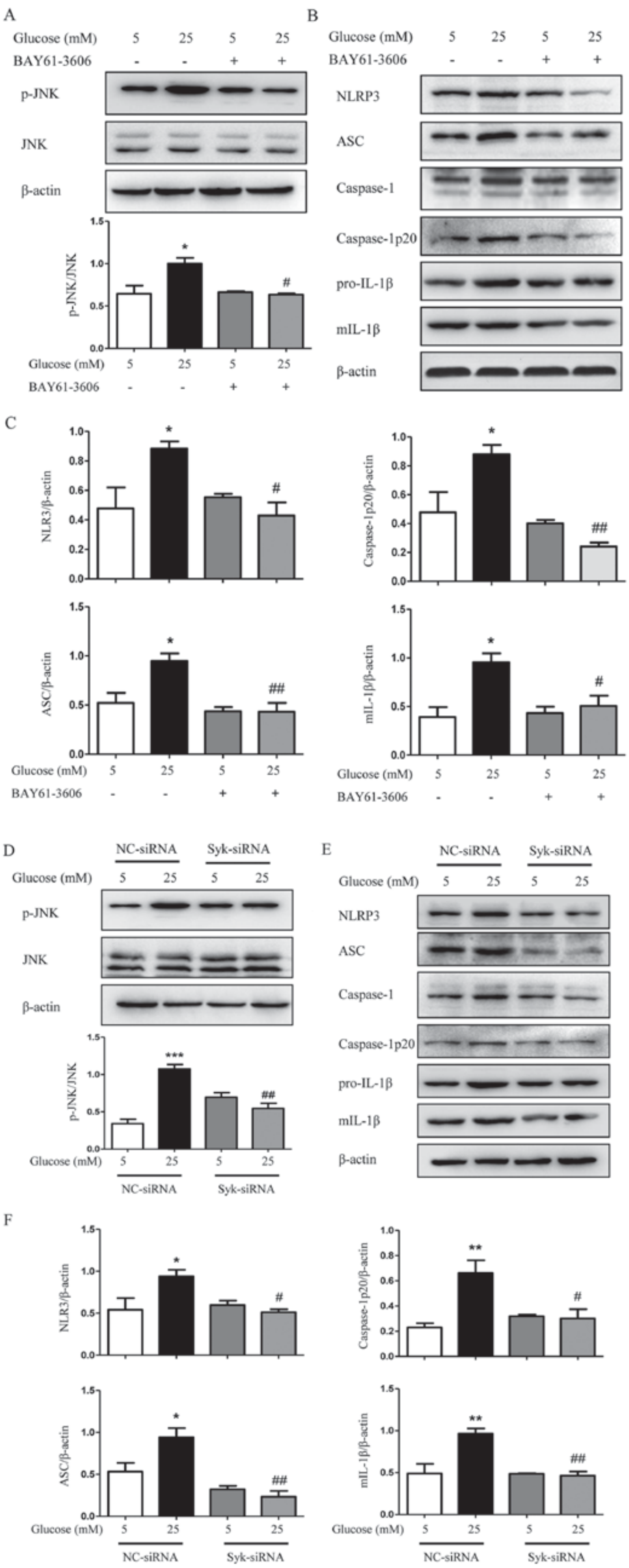

Figure 8. Syk is involved in JNK-dependent NLRP3 inflammasome activation in high glucose-induced RGMCs. (A) Level of p-JNK was examined by western blotting in RGMCs following treatment with BAY61-3606 (1 μM) and analyzed by densitometry. (B) Protein expression level of NLRP3, ASC, caspase-1, caspase-1p20, pro-IL-1β and mIL-1β were examined by western blotting in RGMCs, and (C) analyzed by densitometry. (D) RGMCs transfected with siRNA against Syk were exposed to high glucose condition for 48 h and the phosphorylation of JNK was examined. (E) RGMCs were additionally examined to determine the protein expression levels of NLRP3, ASC, caspase-1, caspase-1p20, pro-IL-1β and mIL-1β by western blotting and (F) analyzed using ImageJ. The data are presented as the mean ± standard error of the mean of three independent experiments. *P<0.05, **P<0.01, ***P<0.001 vs. 5 mM glucose and NC-siRNA. $^{\#}$P<0.05, $^{\#\#}$P<0.01 vs. 25 mM glucose and NC-siRNA by one-way analysis of variance followed by Tukey's post hoc test. RGMCs, rat glomerular mesangial cells; p, phosphorylated; JNK, c-Jun N-terminal kinase; NLRP3, NLR family pyrin domain containing 3; ASC, apoptosis-associated speck-like protein containing a CARD; IL-1β, interleukin 1β; mIL-1β, mature IL-1β; NC, negative control; siRNA, small interfering RNA; Syk, spleen tyrosine kinase.

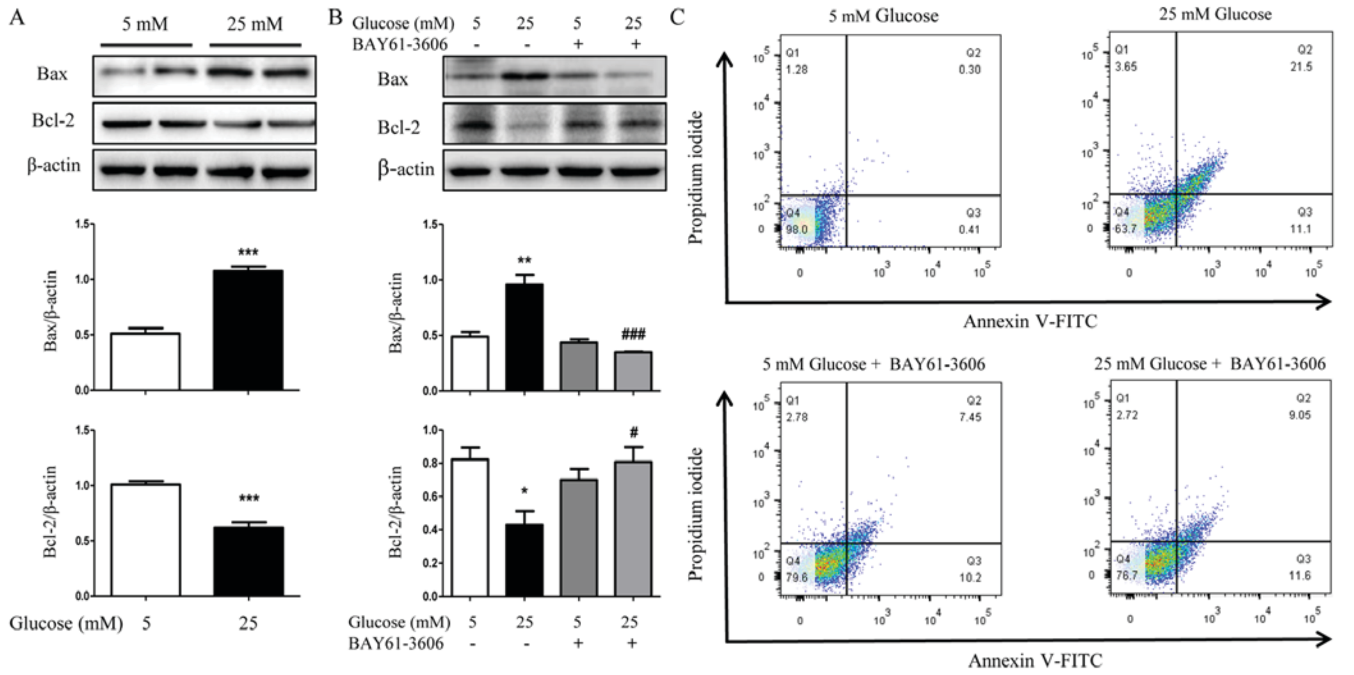

Figure 9. Spleen tyrosine kinase is involved in high glucose-induced apoptosis of HK2 cells. Total protein was extracted from HK2 cells following incubation in different concentrations of (A) glucose and (B) in combination with BAY61-3606, with the protein expression level of Bax and Bcl-2 detected by western blotting and densitometry. (C) Flow cytometry was used to detect apoptosis of HK2 following 24 h exposure to 25 mM glucose with BAY61-3606. All data are presented as the mean ± standard error of at least three independent experiments. *P<0.05, **P<0.01, ***P<0.001 vs. 5 mM glucose using the Student's t-test (for 8A), $^{\#}$P<0.05, $^{\#\#\#}$P<0.001 vs. 25 mM glucose by one-way analysis of variance followed by Tukey's post hoc test (for 8B). Bax, apoptosis regulator Bax; Bcl-2, Bcl-2-associated agonist of cell death; FITC, fluorescein iosthiocyanate.

expression of inflammasome genes, including NLRP3, ASC, caspase-1 and mIL-1β. Similarly, Syk-siRNA reduced the high glucose-induced upregulation of p-JNK and decreased the expression of NLRP3, ASC, caspase-1p20 and mIL-1β in HK2 cells and RGMCs. These results suggest that Syk is a pivotal protein in regulating the pathophysiology of HK2 cells and RGMCs under high glucose condition and Syk inactivation is crucial for protective effects on high glucose-treated HK2 cells and RGMCs.

A previous study demonstrated that high glucose may induce the expression of NLRP3 and pro-caspase-1 in mesangial cells, which leads to the maturation of inflammatory cytokines through proteolysis and tissue inflammation (21). Okada *et al* (11) reported that JNK regulates the NLRP3 inflammasome through the oligomerization of ASC in THP-1 cells. In addition, Syk served a crucial role in mediating NLRP3 stimuli-induced processing of pro-caspase-1 and the consequent activation of caspase-1 in 293T cells, and Syk may directly associate with NLRP3 and ASC, and, interact indirectly with pro-caspase-1 (3). Furthermore, substantial amount evidence supports that Syk is required for activation of JNK signaling, acute neutrophil-mediated glomerular injury and cell death (22,23). Therefore, it was hypothesized that Syk serves a key role in activating JNK signaling, and subsequently induces activation of the NLRP3 inflammasome and mIL-1β during the development of DN. The present study suggested that the Syk/JNK/NLRP3 signaling pathway is a novel signaling pathway involved in DN. Similarly, it was also identified that the Syk/JNK/NLRP3 pathway served an important role in diabetic cardiomyopathy, Syk-siRNA and JNK-siRNA attenuated high glucose-induced upregulation of NLRP3 (data not shown). Thus, this signaling pathway may serve a pivotal role in renal and cardiac function.

Short-term application of inhibitors *in vivo* was usually selected (24,25), and the long-term application of inhibitors (>20 days) is mainly focused on diseases that are accompanied with few complications and little influence on basic metabolism (26,27). The present study was conducted over 4-5 months and it is noteworthy that diabetes deteriorates with time, thus the same dose may exert different effects on diabetic rats at different time points. Therefore, a specific dose of inhibitor, which may be effective in an early stage, may not exert an effect in a later stage. In addition, the internal factors are complex and the application of inhibitors *in vivo* may not be targeted to the kidney. Thus, the effects of Syk and JNK inhibitors in the STZ-induced diabetic rats was not assessed and only the association of Syk, JNK, NLRP3 inflammasome and IL-1β in two types of cells *in vitro* was clarified. Based on the histological examination, diffuse lesions were observed in the diabetic rat kidneys. HK2 cells are frequently used in studies associated with renal inflammatory process (28,29), thus HK2 cells were selected for examination in the present study. Mesangial cells are additionally frequently examined in studies concerning kidney diseases (30,31); therefore, the effect of Syk on RGMCs under high glucose condition was additionally examined. Taken together, it was demonstrated that the Syk signaling pathway was involved in renal tubular injury and glomerular injury by high glucose in the present study.

Previous studies have demonstrated that high glucose rapidly activates Syk, which leads to tyrosine phosphorylation of nuclear factor (NF)-κB inhibitor α and thus activates NF-κB in proximal tubular epithelial cells and glomerular mesangial cells; while deficiency of Syk reverses the effect (32-34), which indicates NF-κB may be involved in the Syk signaling pathway under high glucose conditions. Excessive production of reactive oxygen species (ROS) may promote the generation of various cytokines and stimulate the activation of signaling pathways to affect the bioactivity of renal cells, which may ultimately initiate and participate in the pathogenesis of DN (35). Wei *et al* (36) demonstrated that ROS production leads to activation of mitogen-activated protein kinase 3/1, JNK and NF-κB transcription factor in podocyte. Furthermore, high glucose was able to induce mesangial cell proliferation and fibronectin expression through the JNK/NF-κB/NADPH oxidase/ROS signaling pathways (37) and activate the pathway of ROS/thioredoxin-interacting protein (TXNIP)/NLRP3 inflammasome signaling and results in the release of IL-1β in GMCs (24). TXNIP is implicated in the activation of ROS in rats and humans with DN and closely associated with renal fibrosis (38,39). Thus, the specific roles of inflammatory molecules, including ROS, NF-κB and TXNIP in the Syk/JNK/NLRP3 signaling pathway require further examination in DN. Gasdermin-D (Gsdmd) is a generic substrate for caspase-1 and caspase-4/5/11 and is additionally associated with NF-κB (40,41). The function of Gsdmd in DN requires clarification.

Previous studies suggest that the mechanisms of apoptosis involved in the pathogenesis of DN primarily includes hyperglycemia-mediated oxidative stress-induced apoptosis (42), endoplasmic reticulum stress-induced apoptosis (43), and pro-apoptotic (including Bax and Bcl-2-associated agonist of cell death) and anti-apoptotic (including Bcl-2 and Bcl-xl) Bcl-2 family proteins-mediated apoptosis. However, it was observed that Syk serves an essential role in numerous types of cells, including T-cell non-Hodgkin lymphoma cell lines, human retinoblastoma cells, breast cancer cells, immunocytes and neurons (44-48); therefore, it was investigated whether Syk is involved in the mechanism of apoptosis in high glucose-induced HK2 cells. It was demonstrated that high glucose indeed increased the apoptosis of HK2 cells, and the expression of pro-apoptotic protein Bax was markedly increased; whereas, anti-apoptotic protein Bcl-2 was decreased. The Syk inhibitor eliminated these alterations. All the present data demonstrated that Syk was involved in high glucose-induced apoptosis in HK2 cells; however, the specific mechanism requires further investigation.

In conclusion, the present study demonstrated that the NLRP3 inflammasome acts as a sensor and a regulator of the inflammatory response in DN, resulting in cleavage of pro-caspase-1 and maturation of cytokine IL-1β. The phosphorylation of Syk may predominantly increase the phosphorylation level of JNK and the expression of its downstream molecules, including NLRP3, caspase-1p20, ASC and mIL-1β in high glucose-induced HK2 cells and RGMCs, which may be inhibited by the Syk inhibitor BAY61-3606 or Syk-siRNA. Furthermore, Syk was involved in high glucose-induced apoptosis of HK2 cells. However, the effect of Syk and JNK inhibitors on the STZ-induced diabetic rats was not detected, therefore, the specific mechanism requires further examination. The present results may help to clarify the cellular and molecular basis of the pathogenesis in DN, providing a novel potential target for the treatment of DN.

Acknowledgements

Not applicable.

Funding

The present study was supported by the National Basic Research Program of China (973 Program; grant no. 2015CB553605), National Natural Science Foundation of China (grant nos. 81772252, 31400762 and 81200116), the Natural Science Foundation of Tianjin (grant no. 15JCYBJC49700), the Natural Science Foundation of Tianjin Medical University (grant no. 2014KYQ12), the Key Laboratory of Myocardial Ischemia, Harbin Medical University, Chinese Ministry of Education (grant no. KF201303).

Availability of data and materials

The datasets used during the current study are available from the corresponding author on reasonable request.

Authors' contributions

YaS and YCu conceived the present study and edited the manuscript. YQ and XT performed the experiments and wrote the manuscript. LM was responsible for the detection of renal function of all rats. SL and MX performed the HE and PAS staining, and analyzed data. YCh, YH, PZ and GL participated in the construction of the DN model. YuS and RL were responsible for rat blood glucose monitoring and management of rats. YL and ZQ provided advice and guidance for the implementation of the experiments. All authors discussed the results and implications and commented on the manuscript at all stages.

Ethics approval and consent to participate

All the experimental procedures in the present study were approved by the Animal Care and Welfare Committee of Tianjin Medical University (Hexi, China). The animal use protocol was reviewed and approved by the Animal Ethical and Welfare Committee on 10th January 2017.

Patient consent for publication

Not applicable.

Competing interests

The authors declare that they have no competing interests.

References

1. Wang YW, Wang YG, Luo MY, Wu H, Kong LL, Xin Y, Cui WP, Zhao YJ, Wang JY, Liang G, *et al*: Novel curcumin analog C66 prevents diabetic nephropathy via JNK pathway with the involvement of p300/CBP-mediated histone acetylation. Biochim Biophys Acta 1852: 34-46, 2015.
2. Sun XY, Qin HJ, Zhang Z, Xu Y, Yang XC, Zhao DM, Li XN and Sun LK: Valproate attenuates diabetic nephropathy through inhibition of endoplasmic reticulum stress-induced apoptosis. Mol Med Rep 13: 661-668, 2016.

3. Gao C, Huang W, Kanasaki K and Xu Y: The role of ubiquitination and sumoylation in diabetic nephropathy. Biomed Res Int 2014: 160692, 2014.
4. Prasad N, Gupta P, Jain M, Bhadauria D, Gupta A, Sharma RK and Kaul A: Outcomes of De Novo allograft diabetic nephropathy in renal allograft recipients. Exp Clin Transplant 11: 215-221, 2013.
5. Samra YA, Said HS, Elsherbiny NM, Liou GI, El-Shishtawy MM and Eissa LA: Cepharanthine and Piperine ameliorate diabetic nephropathy inrats:role of NF-κB and NLRP3 inflammasome. Life Sciences 157: 187-199, 2016.
6. Stryker LS: Modifying risk factors: Strategies that work diabetes mellitus. J Arthroplasty 31: 1625-1627, 2016.
7. Hara H, Kohsuke Tsuchiya, Kawamura I, Fang RD, Cuellar EH, Shen YN, Mizuguchi J, Schweighoffer E, Tybulewicz V and Masao Mitsuyama: Phosphorylation of ASC acts as a molecular switch controlling the formation of speck-like aggregates and inflammasome activity. Nat Immunol 14: 1247-1255, 2013.
8. Wada J and Makino H: Inflammation and the pathogenesis of diabetic nephropathy. Clin Sci (Lond) 124: 139-152, 2013.
9. Wang C, Pan Y, Zhang QY, Wang FM and Kong LD: Quercetin and allopurinol ameliorate kidney injury in STZ-treated rats with regulation of renal NLRP3 inflammasome activation and lipid accumulation. PLoS One 7: e38285, 2012.
10. Keller M, Rüegg A, Werner S and Beer HD: Active caspase-1 is a regulator of unconventional protein secretion. Cell 132: 818-831, 2007.
11. Okada M, Matsuzawa A, Yoshimura A and Ichijo H: The lysosome rupture-activated TAK1-JNK pathway regulates NLRP3 inflammasome activation. J Biol Chem 289: 32926-32936, 2014.
12. Yang WS, Chang JW, Han NJ, Lee SK and Park SK: Spleen tyrosine kinase mediates high glucose-induced transforming growth factor-β1 up-regulation in proximal tubular epithelial cells. Exp Cell Res 318: 1867-1876, 2012.
13. Ryan MJ, Johnson G, Kirk J, Fuerstenberg SM, Zager RA and Torok-Seorb B: HK-2: An immortalized proximal tubule epithelial cell line from normal adult human kidney. Kidney Int 45: 48-57, 1994.
14. Gennero I, Fauvel J, Nieto M, Cariven C, Gaits F, Briand-Mésange F, Chap H and Salles JP: Apoptotic effect of sphingosine 1-phosphate and increased sphingosine 1-phosphate hydrolysis on mesangial cells cultured at low cell density. J Biol Chem 277: 12724-12734, 2002.
15. Elsherbiny NM and Al-Gayyar MM: The role of IL-18 in type 1 diabetic nephropathy: The problem and future treatment. Cytokine 81: 15-22, 2016.
16. Qian X, Li XH, Ma FF, Luo SS, Ge RW and Zhu YZ: Novel hydrogen sulfide-releasing compound, S-propargyl-cysteine, prevents STZ-induced diabetic nephropathy. Biochem Biophys Res Commun 473: 931-938, 2016.
17. Pan Y, Zhang XH, Wang Y, Cai L, Ren LQ, Tang LG, Wang JY, Zhao YJ, Wang YG, Liu Q, *et al*: Targeting JNK by a new curcumin analog to inhibit NF-κB-mediated expression of cell adhesion molecules attenuates renal macrophage infiltration and injury in diabetic mice. PLoS ONE 8: e79084, 2013.
18. Jun W and Hirofumi M: Inflammation and the pathogenesis of diabetic Nephropathy. Clin Sci (Lond) 124: 139-152, 2013.
19. Kim SM, Lee SH, Kim YG, Kim SY, Seo JW, Choi YW, Kim DJ, Jeong KH, Lee TW, Ihm CG, *et al:* Hyperuricemia-induced NLRP3 activation of macrophages contributes to the progression of diabetic nephropathy. Am J Physiol Renal Physiol 308: F993-F1003, 2015.
20. Kanellis J, Ma FY, Kandane-Rathnayake R, Dowling JP, Polkinghorne KR, Bennett BL, Friedman GC and Nikolic-Paterson DJ: JNK signaling in human and experimental renal ischaemia/reperfusion injury. Nephrol Dial Transplant 25: 2898-2908, 2010.
21. Feng H, Gu JL, Gou F, Huang W, Gao CL, Chen G, Long Y, Zhou XQ, Yang MJ, Liu S, *et al*: High glucose and lipopolysaccharide prime NLRP3 inflammasome via ROS/TXNIP pathway in mesangial cells. J Diabetes Res 2016: 6973175, 2016.
22. Ryan J, Ma FY, Kanellis J, Delgado M, Blease K and Nikolic-Paterson DJ: Spleen tyrosine kinase promotes acute neutrophil-mediated glomerular injury via activation of JNK and p38 MAPK in rat nephrotoxic serum nephritis. Lab Invest 91: 1727-1738, 2011.
23. Lee CK, Yang Y, Chen C and Liu J: Syk-mediated tyrosine phosphorylation of Mule promotes TNF-induced JNK activation and cell death. Oncogene 35: 1988-1995, 2016.
24. Wu HM, Fang L, Shen QY and Liu RY: SP600125 promotes resolution of allergic airway inflammation via TLR9 in an OVA-induced murine acute asthma model. Mol Immunol 67: 311-316, 2015.
25. Shen H, Wu N, Wang Y, Han X, Zheng Q, Cai X, Zhang H and Zhao M: JNK inhibitor SP600125 attenuates paraquat-induced acute lung injury: An in vivo and in vitro study. Inflammation 40: 1319-1330, 2017.
26. Long AJ, Sampson E, McCarthy RW, Harris CM, Barnard M, Shi D, Conlon D, Caldwell R, Honor D, Wishart N, *et al*: Syk Inhibition induces platelet dependent peri-islet hemorrhage in the rat pancreas. Toxicol Pathol 44: 998-1012, 2016.
27. Llop-Guevara A, Porras M, Cendón C, Di Ceglie I, Siracusa F, Madarena F, Rinotas V, Gómez L, van Lent PL, Douni E, *et al*: Simultaneous inhibition of JAK and SYK kinases ameliorates chronic and destructive arthritis in mice. Arthritis Res Ther 17: 356, 2015.
28. Fu Y, Wang C, Zhang D, Xin Y, Li J, Zhang Y and Chu X: Increased TRPC6 expression is associated with tubular epithelial cell proliferation and inflammation in diabetic nephropathy. Mol Immunol 94: 75-81, 2018.
29. Chen P, Yuan Y, Zhang Ty, Xu B, Gao Q and Guan TJ: Pentosan polysulfate ameliorates apoptosis and inflammation by suppressing activation of the p38 MAPK pathway in high glucose-treated HK2 cells. Int J Mol Med 41: 908-914, 2018.
30. Li J, Bao L, Zha D, Zhang L, Gao P, Zhang J and Wu X: Oridonin protects against the inflammatory response in diabetic nephropathy by inhibiting the TLR4/p38-MAPK and TLR4/NF-κB signaling pathways. Int Immunopharmacol 55: 9-19, 2018.
31. Yang J, Kan M and Wu GY: Bergenin ameliorates diabetic nephropathy in rats via suppressing renal inflammation and TGF-β1-Smads pathway. Immunopharmacol Immunotoxicol 38: 145-152, 2016.
32. Yang WS, Kim JS, Han NJ, Lee MJ and Park SK: Toll-like receptor 4/spleen tyrosine kinase complex in high glucose signal transduction of proximal tubular epithelial cells. Cell Physiol Biochem 35: 2309-2319, 2015.
33. Wang S, Yang Z, Xiong F, Chen C, Chao X, Huang J and Huang H: Betulinic acid ameliorates experimental diabetic-induced renal inflammation and fibrosis via inhibiting the activation of NF-κB signaling pathway. Mol Cell Endocrinol 434: 135-143, 2016.
34. Yang WS, Seo JW, Han NJ, Choi J, Lee KU, Ahn H, Lee SK and Park SK: High glucose-induced NF-kappaB activation occurs via tyrosine phosphorylation of IkappaBaplha in human glomerular endothelial cells: Involvement of Syk tyrosine kinase. Am J Physiol Renal Physio l294: F1065-F1075, 2008.
35. Qi W, Niu J, Qin Q, Qiao Z and Gu Y: Glycated albumin triggers fibrosis and apoptosis via an NADPH oxidase/Nox4-MAPK pathway-dependent mechanism in renal proximal tubular cells. Mol Cell Endocrinol 405: 74-83, 2015.
36. Wei MM, Li ZG, Xiao L and Yang Z: Effects of ROS-relative NF-κB signaling on high glucose-induced TLR4 and MCP-1 expression in podocyte injury. Mol Immunol 68: 261-271, 2015.
37. Zhang LY, Pang SS, Deng B, Qian LH, Chen J, Zou JJ, Zheng JY, Yang LH, Zhang CY, Chen XF, *et al*: High glucose induces renal mesangial cell proliferation and fibronectin expression through JNK/NF-NF-κB/NADPH oxidase/ROS pathway, which is inhibited by resveratrol. Int J Biochem Cell Biol 44: 629-638, 2012.
38. Devi TS, Lee I, Hüttemann M, Kumar A, Nantwi KD and Singh LP: TXNIP links innate host defense mechanisms to oxidative stress and inflammation in retinal muller glia under chronic hyperglycemia: Implications for diabetic retinopathy. Exp Diabetes Res 2012: 438238, 2012.
39. Tan SM, Zhang Y, Cox AJ, Kelly DJ and Qi WE: Tranilast attenuates the up-regulation of thioredoxin-interacting protein and oxidative stress in an experimental model of diabetic nephropathy. Nephrol Dial Transpl 26: 100-110, 2011.
40. Shi JJ, Zhao Y, Wang K, Shi XY, Wang Y, Huang HW, Zhuang YH, Cai T, Wang FC and Shao F: Cleavage of GSDMD by inflammatory caspases determines pyroptotic cell death. Nature 526: 660-676, 2015.
41. Liu ZJ, Lu Gan, Xu YT, Luo D, Ren Q, Song Wu S and Sun C: Melatonin alleviates inflammasome-induced pyroptosis through inhibiting NF-κB/GSDMD signal in mice adipose tissue. J Pineal Res 63, 2017.

42. Pal PB, Sinha K and Sil PC: Mangiferin attenuates diabetic nephropathy by inhibiting oxidative stress mediated signaling cascade, TNFα related and mitochondrial dependent apoptotic pathways in streptozotocin-induced diabetic rats. PLoS One 9: e107220, 2014.
43. Yao F, Li Z, Ehara T, Yang L, Wang D, Feng L, Zhang Y, Wang K, Shi Y, Duan H and Zhang L: Fatty acid-binding protein 4 mediates apoptosis via endoplasmic reticulum stress in mesangial cells of diabetic nephropathy. Mol Cell Endocrinol 411: 232-242, 2015.
44. Wilcox RA, Sun DX, Novak A, Dogan A, Ansell SM and Feldman AL: Inhibition of Syk protein tyrosine kinase induces apoptosis and blocks proliferation in T-cell non-Hodgkin lymphoma cell lines. Leukemia 24: 229-232, 2010.
45. Qiu Q, Yang C, Xiong W, Tahiri H, Payeur M, Superstein R, Carret AS, Hamel P, Ellezam B, Martin B, *et al*: SYK is a target of lymphocyte-derived microparticles in the induction of apoptosis of human retinoblastoma cells. Apoptosis 20: 1613-1622, 2015.
46. Wang WH, Childress MO and Geahlen RL: Syk interacts with and phosphorylates nucleolin to stabilize Bcl-x(L) mRNA and promote cell survival. Mol Cell Biol 34: 3788-3799, 2014.
47. Gobessi S, Laurenti L, Longo PG, Carsetti L, Berno V, Sica S, Leone G and Efremov DG: Inhibition of constitutive and BCR-induced Syk activation downregulates Mcl-1 and induces apoptosis in chronic lymphocytic leukemia B cells. Leukemia 23: 686-697, 2009.
48. Scheib JL, Sullivan CS and Carter BD: Jedi-1 and MEGF10 signal engulfment of apoptotic neurons through the tyrosine kinase Syk. J Neurosci 32: 13022-13031, 2012.